Available online at www.sciencedirect.com

ScienceDirect

Nuclear Physics B 921 (2017) 702–726

NUCLEAR PHYSICS B

www.elsevier.com/locate/nuclphysb

Loop equations and bootstrap methods in the lattice

Peter D. Anderson [a,b,*], Martin Kruczenski [a,*]

[a] *Department of Physics and Astronomy, Purdue U., 525 Northwestern Avenue, W. Lafayette, IN 47907-2036, USA*
[b] *Wigner Research Center for Physics of the HAS, 29–33 Konkoly–Thege Miklós Str., H-1121 Budapest, Hungary*

Received 4 March 2017; accepted 9 June 2017
Available online 17 June 2017
Editor: Leonardo Rastelli

Abstract

Pure gauge theories can be formulated in terms of Wilson Loops by means of the loop equation. In the large-N limit this equation closes in the expectation value of single loops. In particular, using the lattice as a regulator, it becomes a well defined equation for a discrete set of loops. In this paper we study different numerical approaches to solving this equation. Previous ideas gave good results in the strong coupling region. Here we propose an alternative method based on the observation that certain matrices $\hat{\rho}$ of Wilson loop expectation values are positive definite. They also have unit trace ($\hat{\rho} \succeq 0, \mathrm{Tr}\hat{\rho} = 1$), in fact they can be defined as reduced density matrices in the space of open loops after tracing over color indices and can be used to define an entropy associated with the loss of information due to such trace $S_{WL} = -\mathrm{Tr}[\hat{\rho} \ln \hat{\rho}]$. The condition that such matrices are positive definite allows us to study the weak coupling region which is relevant for the continuum limit. In the exactly solvable case of two dimensions this approach gives very good results by considering just a few loops. In four dimensions it gives good results in the weak coupling region and therefore is complementary to the strong coupling expansion. We compare the results with standard Monte Carlo simulations.

1. Introduction

Gauge theories are of fundamental importance for our understanding of Nature but many of their properties are still mysterious, for example in pure gauge theories, the phenomenon of con-

* Corresponding author.
E-mail addresses: ander324@purdue.edu (P.D. Anderson), markru@purdue.edu (M. Kruczenski).

http://dx.doi.org/10.1016/j.nuclphysb.2017.06.009

finement is still not fully understood. Even further, the AdS/CFT correspondence [1] has shown that gauge theories in the strongly coupled regime can be described equally well in terms of string theory in a higher dimensional space. That means that certain gauge theories contain quantum gravity, emergent space-time and strings as bound states. Fundamental to this understanding is the relation of gauge theories and string theory in the limit of a large number of colors as envisioned by 't Hooft [2]. In such relation, exemplified by AdS/CFT, the string theory description is completely in terms of gauge invariant operators. In fact the gauge symmetry is not a symmetry of the dual theory in accordance with the usual understanding that a gauge symmetry is a manifestation of redundant degrees of freedoms that have to be eliminated. Taken to its logical conclusion, the principle of gauge invariance cannot be used as the basis to construct such a theory and perhaps more ideas are needed to understand the fundamental principles lying behind gauge theories.

For these reasons it is natural to study gauge invariant formulations of gauge theories. In fact it is known that gauge theories can be formulated entirely in terms of Wilson loops. In particular, in the large-N limit Wilson loops obey an equation that closes in the expectation value of single Wilson loops. This is known as the loop equation [3,4] or the Migdal–Makeenko equation. For finite N the equation is also valid but closes in the expectation value of disconnected (*i.e.* multitrace) Wilson loops. Since it is not clear how to renormalize the loop equation it can be better studied perturbatively or in the lattice. Motivated by this, here we discuss different numerical and analytical methods to study the loop equation in the lattice.

Although, as we argued, this equation is of great importance there does not seem to be many studies on how to solve it. A notable exception is the very interesting work by Marchesini [5] where a formal solution and a numerical approach to solve the loop equation was proposed. We discuss this approach in detail but unfortunately it seems restricted to the strongly coupled regime, moreover, and the known numerical results are for the 2d case. The method we propose is based on the observation that certain matrices constructed of Wilson loop expectation values are positive definite. They can be thought of as reduced density matrices in the space of open loops after tracing over color indices. Imposing this extra condition allow us to select valid solutions of the loop equations. We call this approach a bootstrap approach since it uses general positivity properties of the theory to impose bounds on the solutions and also since imposing positive definiteness is an important part of the recently developed and highly successful conformal bootstrap program [6,7].[1] The bounds we impose are for the expectation value of the energy. In two dimensions such bounds constrain the solution to be equal to the exact solution with high degree of accuracy. In four dimensions the bounds are less restrictive (due to larger computational complexity) but we can resort to a simple approximation, at small coupling we minimize the expectation value of the energy subject to the constraints, whereas at large coupling the entropy should be maximized. This gives results which are in good agreement with simulations and a reasonable approximation to the coupling where the transition occurs. The weak coupling region is well described by this method although, at the moment, this is not enough to understand the continuum limit.

For future work, it seems of great interest to apply this method to $\mathcal{N} = 4$ SYM in order to make contact with the AdS/CFT correspondence. In this paper we take a few initial steps in this

[1] We want to clarify however, that the ideas discussed here do not seem to have any relation with conformal symmetry. Perhaps closer is the idea of applying the bootstrap method to non-conformal theories [8] but we do not know of any direct relation with the present work.

direction by briefly considering the bosonic sector of $\mathcal{N} = 4$ SYM but leave a detailed study for future work.

It is interesting to note that the relevance of the extra positivity conditions at weak coupling was already observed [9] in the collective field method of Jevicki and Sakita [10]. Using the Kogut–Susskind approach a Lattice Hamiltonian in loop space was derived and numerically studied in [9]. See also the related work by Yaffe [11] using coherent states.

This paper is organized as follows, in the next section we review the derivation of the loop equation and summarize the main ideas presented in this paper, following that we consider in great detail the two dimensional case since its solution is known exactly and can be used to test various approaches very easily. Afterwards, we apply those ideas to the four dimensional case and show that our numerical approach gives a good understanding of the gauge theory in the small coupling regime relevant for the continuum limit. Finally we describe a numerical simulation used to validate the results, discuss briefly the case of $\mathcal{N} = 4$ SYM and conclude with a summary of the results and possible extensions and improvements.

2. Lattice gauge theory, a brief summary

In this section we consider a four dimensional $SU(N)$ gauge theory in an infinite cubic lattice with Wilson action and briefly review known results for the large N limit including the derivation of the loop equation. There is an extensive literature on the subject, we mostly follow the classic review [12] and the book [13] as regards to the loop equation.

2.1. Lattice action and known results

The system we consider is a cubic lattice where to each oriented link is associated a matrix $U_\mu \in SU(N)$. To the same link with opposite orientation we associate the matrix $U_{\bar{\mu}} = U_\mu^\dagger$. The action is the Wilson action

$$S = -\frac{N}{2\lambda} \sum_P \mathrm{Tr} U_P \ , \tag{1}$$

where the sum is over all oriented plaquettes P. Here U_P is the product of the four matrices associated with the plaquette and oriented means that we sum the trace of both possible orientation so that the action is real. The partition function is

$$Z = \int \prod_{\vec{x},\mu} dU_\mu(\vec{x}) \, e^{-S}. \tag{2}$$

In four dimensions, for $N \geq 4$ numerical results indicate that this theory has a first order phase transition as a function of λ [12]. In the large-N limit the transition occurs at $\lambda_c = 1.3904$, as computed using the Twisted Eguchi–Kawai (TEK) model [14]. The nature of the transition is easily understood by considering the partition function in eq. (2) as defining a classical four dimensional statistical system with Hamiltonian

$$H = -\frac{N}{2} \sum_P \mathrm{Tr} U_P \ , \tag{3}$$

and temperature $T = \lambda$. At small temperature $\lambda \to 0$ we minimize the energy, *i.e.* the links U_μ fluctuate around gauge trivial configurations. At large temperature $\lambda \to \infty$ the entropy should be

maximized and the links variables U_μ explore all possible values with equal probability. Thus, the transition is a typical transition between ordered and disordered states.

The large coupling phase is confining and easily studied analytically in terms of a strong coupling expansion already proposed by Wilson [15]. On the other hand the continuum limit is obtained in the region $\lambda \to 0$ which is more difficult to study. The main observable is the Wilson loop expectation value, a real number associated with a closed path in the lattice and defined as

$$\mathcal{W}_\mathcal{C} = \frac{1}{Z} \int \prod_{\vec{x}\mu} dU_\mu(\vec{x}) \; \frac{1}{N} \mathrm{Tr}(U_{\mu_1} \dots U_{\mu_L}) e^{-S} \,, \tag{4}$$

where inside the trace we multiplied in cyclic order all the matrices associated to the given path $\mathcal{C} = \{\mu_1 \mu_2 \dots \mu_L\}$. The simplest one is the null loop $\mathcal{W}_0 = 1$, namely just a point and the plaquette that we denote as $u = \mathcal{W}_1$ that is related to the average energy per site: $\frac{E}{VN^2} = -6u$. It should be emphasized however that the main physical interest lies in the continuum limit that appears in the $\lambda \to 0$ region. In practice one has to show that large loops obey the area law in the weak coupling phase, a result that cannot be obtained by perturbation theory and can only be found by extrapolation of numerical simulations. In any case, our intention here is to study this system purely in terms of gauge invariant operators, namely with no reference to the variables U_μ. For that reason we review now the derivation of the loop equation.

2.2. The loop equation

The loop equation is a direct consequence of the Schwinger–Dyson equation associated with a link of the lattice [3,4,13]. We reproduce its derivation here, first to introduce the notation, and second because for other theories the derivation will be done just by analogy to this one. Consider then a point $\vec{x}$ in a cubic lattice of dimension d and a given link $\mu = 1, \dots, d$, and perform the following change of variables

$$U_\mu \to (1 + i\epsilon) U_\mu, \quad U_\mu^\dagger \to U_\mu^\dagger (1 - i\epsilon), \quad \epsilon^\dagger = \epsilon, \quad \mathrm{Tr}\epsilon = 0 \,. \tag{5}$$

The variation of the Wilson action (1) is

$$\delta S = -\frac{N}{2\lambda} \sum_{\pm \nu \neq \mu} \Big(i\epsilon_{ab} W^{ab}\{\mu\nu\bar{\mu}\bar{\nu}\} - i\epsilon_{ab} W^{ba}\{\nu\mu\bar{\nu}\bar{\mu}\} \Big) \,, \tag{6}$$

where $W^{ab}\{\mu\nu\bar{\mu}\bar{\nu}\}$ indicates a Wilson line made of four links starting and ending at $\vec{x}$ and following the directions $\{\mu\nu\bar{\mu}\bar{\nu}\}$ where the bar indicates that the link is traversed in the opposite direction as μ. Let us perform this change of variables in the integral

$$\int \mathcal{D}U \; \delta_\epsilon \Big(e^{-S} \; W_{\vec{x}}^{ab}\{\mu, \hat{\mathcal{C}}\} \Big) = 0 \,, \tag{7}$$

where $W_{\vec{x}}^{ab}\{\mu, \hat{\mathcal{C}}\}$ indicates a Wilson line starting at point $\vec{x}$ in direction μ and then coming back to $\vec{x}$ along some given path $\hat{\mathcal{C}}$ that in principle may pass again through the same link $\vec{x}, \mu$ in the positive or negative direction. Since the measure is invariant under this change of variables, it follows that

$$\langle -\delta_\epsilon S \; W_{\vec{x}}^{ab} \rangle + \langle \delta_\epsilon W_{\vec{x}}^{ab} \rangle = 0 \,. \tag{8}$$

Explicitly

$$\frac{iN}{2\lambda}\langle \sum_{\pm\nu\neq\mu}\Big(\epsilon_{cd}W^{dc}\{\mu\nu\bar{\mu}\bar{\nu}\}-\epsilon_{cd}W^{dc}\{\nu\mu\bar{\nu}\bar{\mu}\}\Big)W^{ab}_{\vec{x}}\{\mu,\hat{\mathcal{C}}\}\rangle + i\epsilon^{ad}\langle W^{db}_{\vec{x}}\rangle$$
$$+\langle\sum_{j_+=1}^{n_+} i\,W^{ac}_{\vec{x}\vec{x}+}\epsilon^{cd}W^{db}_{\vec{x}+\vec{x}}\rangle-\langle\sum_{j_-=1}^{n_-} i\,W^{ac}_{\vec{x}\vec{x}-}\epsilon^{cd}W^{db}_{\vec{x}-\vec{x}}\rangle=0\,, \tag{9}$$

where the terms in the last line come from the possibility that the path goes through the same link again either in the same direction (n_+ times), or opposite direction (n_- times). These terms are call self-intersection terms but notice that self-intersection in this context means that the loop goes through the same link more than once (in either direction) and not merely through the same vertex. Using that this identity is valid for any traceless hermitian ϵ and after some manipulations we obtain

$$\frac{N}{2\lambda}\sum_{\pm\nu\neq\mu}\langle W_{\vec{x}}\{\mu\nu\bar{\mu}\bar{\nu}\mu\hat{\mathcal{C}}\}-W_{\vec{x}}\{\nu\mu\bar{\nu}\hat{\mathcal{C}}\}\rangle+N\langle W_{\vec{x}}\rangle$$
$$+\sum_{j_+=1}^{n_+}\langle W_{\vec{x}\vec{x}+}W_{\vec{x}+\vec{x}}\rangle-\sum_{j_-=1}^{n_-}\langle W_{\vec{x}\vec{x}-}W_{\vec{x}-\vec{x}}\rangle= \tag{10}$$
$$\frac{1}{2\lambda}\langle\sum_{\pm\nu\neq\mu}W_{\vec{x}}\{\mu\nu\bar{\mu}\bar{\nu}\}W_{\vec{x}}-W_{\vec{x}}\{\nu\mu\bar{\nu}\bar{\mu}\}W_{\vec{x}}\rangle+\frac{1}{N}(n_+-n_-+1)\langle W_{\vec{x}}\rangle\,,$$

a useful form of the loop equation associated with each link of the loop. In the large N limit, we divide both sides by N^2 and get

$$\frac{1}{2\lambda}\sum_{\pm\nu\neq\mu}\mathcal{W}_{\vec{x}}\{\mu\nu\bar{\mu}\bar{\nu}\mu\hat{\mathcal{C}}\}-\mathcal{W}_{\vec{x}}\{\nu\mu\bar{\nu}\hat{\mathcal{C}}\}+\mathcal{W}_{\vec{x}}+\sum_{j_+=1}^{n_+}\mathcal{W}_{\vec{x}\vec{x}+}\mathcal{W}_{\vec{x}_+\vec{x}}-\sum_{j_-=1}^{n_-}\mathcal{W}_{\vec{x}\vec{x}-}\mathcal{W}_{\vec{x}-\vec{x}}=0\,, \tag{11}$$

where we defined

$$\mathcal{W}\{\mathcal{C}\}=\frac{1}{N}\langle W\{\mathcal{C}\}\rangle\,, \tag{12}$$

and used the large N factorization property [16]

$$\frac{1}{N^2}\langle W\{\mathcal{C}_1\}W\{\mathcal{C}_2\}\rangle=\mathcal{W}\{\mathcal{C}_1\}\,\mathcal{W}\{\mathcal{C}_2\}+\mathcal{O}(\frac{1}{N^2})\,. \tag{13}$$

The different terms in the result have a very simple graphical interpretation as seen in Figs. 1, 2. The link $\vec{x},\mu$ appears in the action in several plaquettes. Each of these plaquettes is connected to the loop as in the figure, when the orientations are opposite, we include a minus sign. Also the action comes with a coefficient $\frac{N}{2\lambda}$. Summing over all links we get the loop equation that we schematically write as

$$-\frac{1}{NL}S*\mathcal{W}+\mathcal{W}+\frac{1}{L}\sum_i\sigma_i\mathcal{W}_{1i}\mathcal{W}_{2i}=0\,, \tag{14}$$

where L denotes the length of the loop, $S*\mathcal{W}$ denotes all possible intersections between the loops appearing in the Wilson loop (at a fixed position) and those appearing in the action. The last term

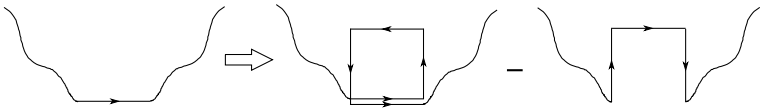

Fig. 1. Intersection with the action $S * W$ term. In this case the action is simply given by a plaquette. Curvy lines represent schematically the rest of the loop.

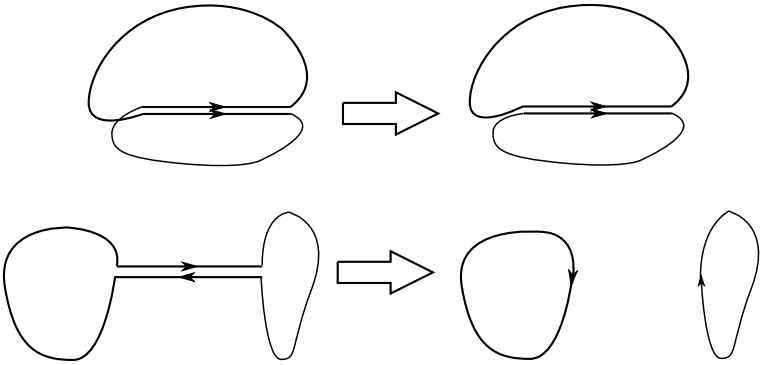

Fig. 2. Self intersection terms. It only appears if the Wilson loop traverses the same link more than once (in the same or opposite directions). The first type gives a positive contribution, the second one a negative one.

is a sum over all self-intersections with a sign σ_i depending on the orientation of the intersection and $\mathcal{C}_1$ and $\mathcal{C}_2$ denote the two loops in which the original loop splits when reconnecting at that self-intersection (see Fig. 2). In this form the loop equation is valid for any action given by a sum of Wilson loops. Therefore, we can give a linear combination of loops as the action and the reconnection procedure determines completely the loop equation without any reference to matrices, gauge invariance etc.

For mathematical manipulations it is convenient to enumerate the loops in a list, where we eliminate redundancy due to rotations, translations, cyclic permutations and opposite orientations. The first few elements of the list are in Fig. 3. Then we can write the loop equation in the form

$$\mathbb{K}_{i\to j}\mathcal{W}_j + 2\lambda\mathcal{W}_i + 2\lambda\mathbb{C}_{i\to jk}\mathcal{W}_j\mathcal{W}_k = \delta_{i1}\ , \tag{15}$$

where $\mathcal{W}_i$ denotes the expectation value of loop i, $\mathbb{K}_{i\to j}$ is a matrix indicating that loop i converts into loop j by the reconnection procedure of the action with a weight depending on how many different ways we can get j and divided by the length of the loop L. The tensor $C_{i\to jk}$ is the self-intersection term and indicates that Wilson loop i splits into jk with an appropriate coefficient. For example, for the plaquette we get

$$-\mathcal{W}_0 - \mathcal{W}_2 - 4\mathcal{W}_3 + \mathcal{W}_{17} + \mathcal{W}_{20} + 4\mathcal{W}_{21} + 2\lambda\mathcal{W}_1 = 0\ . \tag{16}$$

2.3. Extra equations

From the derivation of the previous subsection it is clear that we can get more equations than just the loop equation. First we can obtain individual Schwinger–Dyson equations for each link. Given two links that do not belong to a self-intersection, the difference between their respective

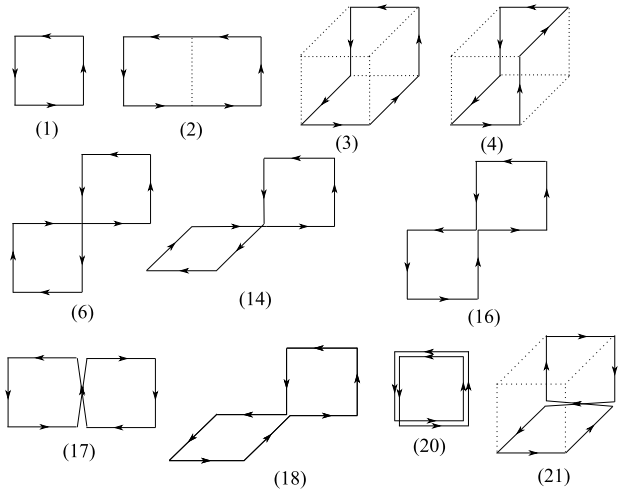

Fig. 3. We construct a numbered list of Wilson loops up to translations, rotations and cyclic permutations. Some examples are in the figure.

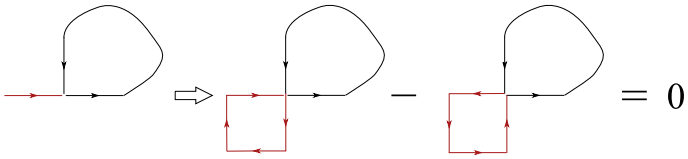

Fig. 4. Loop Equation associated with a link (in red) not in the loop but sharing a vertex with the loop. The equation is linear and independent of the coupling. It can be thought as a constraint. (For interpretation of the references to color in this figure, the reader is referred to the web version of this article.)

equations is linear and independent of λ. Other linear lambda-independent equations can be obtained from the equations associated to links that touch the loop but do not belong to it (see Fig. 4). All these equations are linear and λ-independent and we denote them as constraints since do not have information on the coupling:

$$B_{ij}\mathcal{W}_j = 0\,. \tag{17}$$

An example is:

$$\mathcal{W}_2 + \mathcal{W}_6 + 4\mathcal{W}_{14} - \mathcal{W}_{16} - \mathcal{W}_{17} - 4\mathcal{W}_{18} = 0\,. \tag{18}$$

They should also be imposed since they restrict the possible values of the Wilson loops.

2.4. Positivity constraints

Finally, it is important to observe that there are certain positive definite matrices whose entries are the expectation values of the Wilson loops. They are very easy to construct. Indeed, take two points x_1 and x_2 on the lattice and a set of open Wilson lines $\mathcal{C}_\ell$, $\ell = 1 \ldots L$ going from x_1 to x_2, see Fig. 5. Consider an arbitrary configuration of the lattice (namely of matrices U_μ associated

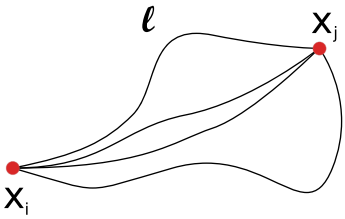

Fig. 5. A given set of open loops connecting two points in space define a matrix of closed loop expectation values $\hat{\rho}_{\ell\ell'} = \frac{1}{NL}\langle \mathrm{Tr}\left[\left(U^{(\ell)}\right)^\dagger U^{(\ell')}\right]\rangle$ that has to be positive definite, $\hat{\rho} \succeq 0$.

with each link) and compute the matrices $U^{(\ell)}$ associated with the curves ℓ. Given an arbitrary set of coefficients c_ℓ we define

$$A = \sum_{\ell=1}^{L} c_\ell U^{(\ell)} \,, \tag{19}$$

and since $\mathrm{Tr} A^\dagger A \geq 0$ for any c_ℓ, and using that the average of a non-negative quantity is non-negative, we find that the matrix of Wilson loop expectation values

$$\hat{\rho}_{\ell\ell'} = \frac{1}{NL}\langle \mathrm{Tr}\left[\left(U^{(\ell)}\right)^\dagger U^{(\ell')}\right]\rangle \,, \tag{20}$$

is positive semi-definite for any set of open loops and any two points $x_{1,2}$. This is true in the continuum and in the lattice, furthermore it does not require the matrices $U^{(\ell)}$ to be unitary, only that the reverse path is associated with $(U^{(\ell)})^\dagger$. For the lattice case we choose different pairs of points and list all possible open loops up to a certain length. In this way we construct a set of matrices that have to be positive definite, its structure depends on the topology of the lattice but not on the action and therefore they contain important kinematic information on the loops.

In the $SU(N)$ gauge theory, the $U^{(\ell)}$ matrices are unitary and the diagonal elements are $\hat{\rho}_{\ell\ell} = \frac{1}{L}$ implying $\mathrm{Tr}\hat{\rho} = 1$. Therefore $\hat{\rho}$ has properties of a density matrix. Indeed, we can write its definition as

$$\hat{\rho}_{\ell\ell'} = \frac{1}{NL}\sum_{ab} (U^{(\ell)})^*_{ab} U^{(\ell')}_{ab} \,. \tag{21}$$

Namely, if we take the collection of all matrices $U^{(\ell)}$, the matrix $\hat{\rho}$ traces over the color indices, the associated entropy $S_{WL} = -\mathrm{Tr}\hat{\rho}^{(L)} \ln \hat{\rho}^{(L)}$ measures the information loss due to such tracing. In the small coupling phase the matrices $U^{(\ell)}$ are all close to the identity (up to gauge transformations) and therefore S_{WL} is small, in the large coupling phase the matrices fluctuate over all possible values and S_{WL} is large. Thus, S_{WL} measures the disorder of the system.

To conclude this section let us notice a few more results regarding these matrices that can be derived independently of the action that we use to average the Wilson loops.

- If we take $x_1 = x_2$ and two loops that start and end at x_1 and share the first link, see Fig. 5, we can construct the matrix

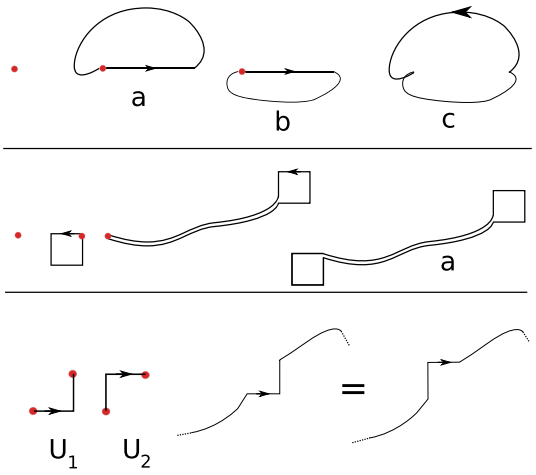

Fig. 6. Three examples of applying the positivity constraints. The red dots denote a point where an open line starts and/or ends. The first one gives $(\mathcal{W}_a - \mathcal{W}_b)^2 \leq (1 - \mathcal{W}_c)(1 + \mathcal{W}_c - 2\mathcal{W}_a\mathcal{W}_b)$, the second $\mathcal{W}_a \geq 2u^2 - 1$, where u is the plaquette, and the third one implies that if $u = 1$ then for all configurations the matrices $U_{1,2}$ associated with the two paths are equal $U_1 = U_2$ and then all loops are equal to one.

$$\hat{\rho} = \begin{pmatrix} 1 & \mathcal{W}_a & \mathcal{W}_b \\ \mathcal{W}_a & 1 & \mathcal{W}_c \\ \mathcal{W}_b & \mathcal{W}_c & 1 \end{pmatrix} \succeq 0 \;\Rightarrow\; 0 \leq (\mathcal{W}_a - \mathcal{W}_b)^2 \leq (1 - \mathcal{W}_c)(1 + \mathcal{W}_c - 2\mathcal{W}_a\mathcal{W}_b) \,, \tag{22}$$

where $\mathcal{W}_c$ is the intersection of $\mathcal{W}_a$ and $\mathcal{W}_b$ as in the figure. In particular, if a is a plaquette, c is any loop that appears in the Laplacian of b, namely in the loop equation for b.

- Another example is a long loop a made out of two plaquettes connected by a long path (Fig. 5). Cutting this loop in two as in the figure and using the same procedure we obtain

$$\mathcal{W}_a \geq 2u^2 - 1 \,, \tag{23}$$

where u is the expectation value of the plaquette. This means that, if the expectation value of the plaquette is close to one, there are arbitrary long loops that are also close to one.

- Finally notice that, if the matrix $\hat{\rho}$ has a zero eigenvalue, namely it is in the boundary of the allowed region, then for a given set of coefficients $\hat{c}_\ell$ in eq. (19) the matrix A vanishes and this in turn implies an infinite set of linear equations for loops that contain the given open paths. Namely, taking an arbitrary path $\mathcal{C}_0$ from x_j to x_i we get

$$\langle \sum_{\ell=1}^{L} \hat{c}_\ell \mathrm{Tr}\left[U_0 U^{(\ell)}\right] \rangle = 0 \,. \tag{24}$$

As a simple example, let us show that if the plaquette is one ($u = 1$) then all loops are equal to one. Indeed, take two paths that build a plaquette as in Fig. 6, we get the matrix

$$\hat{\rho} = \begin{pmatrix} 1 & u \\ u & 1 \end{pmatrix} \succeq 0 \;\Rightarrow\; |u|^2 \leq 1 \,, \tag{25}$$

as expected. However, if the bound is saturated, *i.e.* $u = 1$ then the matrix associated with the zero eigenvalue should vanish. Namely $A = U_1 - U_2 = 0$. Since we can use this in any loop

it simply means that, for any loop, performing a move such as the one in the same figure does not change its expectation value. Since any loop can be reduced to a point by such moves, then all loops are equal to one.

Having reviewed some simple facts about the Lattice theory, let us now discuss methods to numerically solve the loop equation. We start with the simple case of two dimensions since we can compare with exact results.

3. Two dimensional lattice

The two dimensional system is a well known system that can be solved exactly even in the large-N limit [17]. In this paper we use it to test our numerical method before extending it to the more challenging case of four dimensions. In axial gauge, $U_0 = \mathbb{I}$, the two dimensional case reduces to the single plaquette:

$$Z = \int dU e^{\frac{N}{2\lambda}\mathrm{Tr}(U+U^\dagger)} \,. \tag{26}$$

The Wilson loops can be labeled by an integer

$$\mathcal{W}_n = \frac{1}{N}\langle \mathrm{Tr} U^n \rangle \,. \tag{27}$$

The large N limit was studied by Gross and Witten as well as Wadia [17] using the saddle point of an effective action for $\rho(\theta)$, the density of eigenvalues $e^{i\theta}$ of U in the interval $\theta \in [-\pi, \pi]$. Notice that $\rho(\theta)$ is also the generating function for the Wilson loops

$$\mathcal{W}_n = \frac{1}{2\pi}\int_{-\pi}^{\pi} e^{in\theta}\rho(\theta)\, d\theta \quad \Rightarrow \quad \rho(\theta) = 1 + 2\sum_n \mathcal{W}_n \cos(n\theta) \,. \tag{28}$$

The result for the plaquette (and therefore the energy) is [17]

$$\mathcal{W}_1 = u = \begin{cases} 1 - \frac{\lambda}{2} & \lambda \le 1 \\ \frac{1}{2\lambda} & \lambda \ge 1 \end{cases} \tag{29}$$

from where it is seen that there is a third order phase transition at $\lambda = 1$. Later Friedan [18] obtained the same result using the loop equation, that in this case reads:

$$\mathcal{W}_{n+1} - \mathcal{W}_{n-1} + 2\lambda\mathcal{W}_n + 2\lambda\sum_{p=1}^{n-1}\mathcal{W}_p\mathcal{W}_{n-p} = 0, \quad n > 0 \,, \tag{30}$$

The positivity constraint described in section 2.4 can be obtained by taking $U^{(\ell)} = U^\ell$ and reduce to the condition that

$$\hat{\rho}^{(L)} = \frac{1}{L}\begin{bmatrix} \mathcal{W}_0 & \mathcal{W}_1 & \mathcal{W}_2 & \dots & \mathcal{W}_L \\ \mathcal{W}_1 & \mathcal{W}_0 & \mathcal{W}_1 & \dots & \mathcal{W}_{L-1} \\ \mathcal{W}_2 & \mathcal{W}_1 & \mathcal{W}_0 & \dots & \mathcal{W}_{L-2} \\ \vdots & \vdots & \vdots & \ddots & \vdots \\ \mathcal{W}_L & \mathcal{W}_{L-1} & \mathcal{W}_{L-2} & \dots & \mathcal{W}_0 \end{bmatrix} \succeq 0 \,, \tag{31}$$

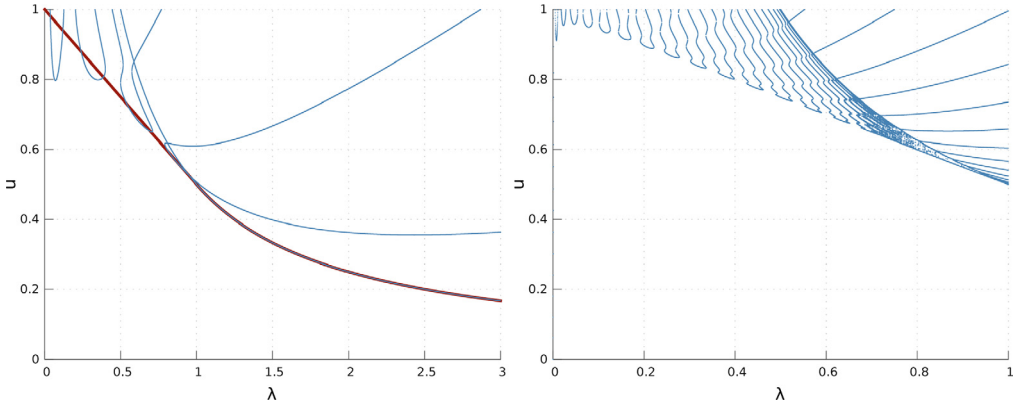

(a) $L = 10$ (b) $L = 49$

Fig. 7. Solution to the 2D loop equation by setting to zero loops larger than L. In fig. (a) the strong coupling is correctly described whereas in the region $\lambda < 1$ the results are not good. Going to $L = 49$, fig.(b), the small coupling solution appears as one of the roots but not for every value of λ.

where $\hat{\rho} \succeq 0$ indicates that $\hat{\rho}$ is positive semi-definite. Mathematically, eq. (31) is the definition of a Toeplitz matrix $\hat{\rho}^{(L)}$

$$\hat{\rho}^{(L)}_{ij} = \frac{1}{L}\mathbb{T}[\mathcal{W}_0, \ldots, \mathcal{W}_L]_{ij} = \frac{1}{L}\mathcal{W}_{|i-j|} \,. \tag{32}$$

A useful comment is that the Toeplitz matrix is associated with the Fourier coefficients of the eigenvalue density $\rho(\theta)$ of U. In such case one can use Szegö theorems [19] to compute limits of functions of the eigenvalues of $\hat{\rho}^{(L)}$ by using integrals of the eigenvalue density:

$$\lim_{L\to\infty} \frac{1}{L}\sum_{j=1}^{L} F(L\,\mu_j^{(L)}) = \frac{1}{2\pi}\int_{-\pi}^{\pi} F(\rho(\theta))\,d\theta \,, \tag{33}$$

where $\mu^{(L)}_{j=1\ldots L}$ are the eigenvalues of $\hat{\rho}^{(L)}$ and $\rho(\theta)$ is the eigenvalue density (28).

3.1. Numerical solution

In two dimensions the loop equation (30) can be understood as a recursion relation that determines all loops if $\mathcal{W}_0 = 1$ and $\mathcal{W}_1 = u$ are given. However, u is not determined and therefore there are an infinite number of solutions, one for each value of u. In [5] Marchesini proposed to truncate the equations by setting $\mathcal{W}_{L+1} = 0$ for some given L, thus obtaining a polynomial equation for u:

$$\mathcal{W}_{L+1} = P_L(\lambda, u) = 0 \,. \tag{34}$$

The roots of the polynomial give the possible values of u. This polynomial has always a root $u = \frac{1}{2\lambda}$ that corresponds to the strong coupling solution. For small λ other solutions appear but the weak coupling solution is only reproduced in a very approximate way and for very large loops, see Fig. 7.

Instead of setting $\mathcal{W}_{L+1} = 0$ our proposal is to let it fluctuate over its allowed range $-1 \leq \mathcal{W}_{L+1} \leq 1$ and determine the range of variation of the plaquette expectation value $\mathcal{W}_1 = u$.

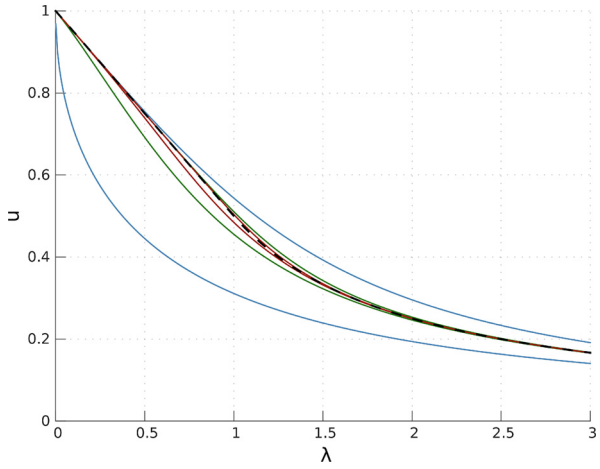

Fig. 8. Upper and lower bounds to the plaquette expectation value by imposing positivity of $\hat{\rho}^{(L)}$ for $L = 4$ (blue), $L = 6$ (green) and $L = 8$ (red). The dashed line is the exact answer always contained between the two bounds that almost coincide for $L = 8$. For small coupling the upper bound agrees with the exact answer even for $L = 4$. (For interpretation of the colors in this figure, the reader is referred to the web version of this article.)

The two conditions that need to be imposed are the validity of the loop equation up to L and the positivity constraint $\hat{\rho}^{(L)} \succeq 0$. In the allowed region, $\hat{\rho}^{(L)} \succ 0$, all eigenvalues of $\hat{\rho}^{(L)}$ are positive. As we vary u, we reach the boundary of the allowed region when an eigenvalue vanishes, namely $\det \hat{\rho}^{(L)} = 0$. This determinant is a polynomial in u and therefore the roots of such polynomial determine the analytical bounds of the allowed region, for given L. Again we increase L by one in each step contracting the allowed region every time. The results are displayed in Fig. 8 where we can see that already for lower values of L the approximation is very good. For reference we give

$$\det \hat{\rho}^{(L=4)} = 4\lambda^2 \left[u^2(u^2-1)^2 - (u^2 + 2\lambda u - 1)^2 \right] \tag{35}$$

The two roots of this polynomial contained in the interval $[0, 1]$ correspond to the blue curves in Fig. 8.

3.2. *Effective action, numerical solution*

In two dimension it is possible to side step the loop equation and use an effective action for the Wilson loop. This helps clarify the role of the positivity constraints but cannot be easily extended to four dimensions. In [17], the following effective action for the eigenvalue density was constructed:

$$S = -\frac{1}{2\pi\lambda} \int_{-\pi}^{\pi} d\theta \rho(\theta) \cos\theta - \frac{1}{4\pi^2} \fint_{-\pi}^{\pi} \fint_{-\pi}^{\pi} d\theta d\theta' \rho(\theta)\rho(\theta') \ln \left| \sin\left(\frac{\theta - \theta'}{2}\right) \right| , \tag{36}$$

where $\fint$ indicates principal part. Using [20]

$$\fint_{-\pi}^{\pi} \cos n\theta \ln|\sin\frac{\theta}{2}| = -\frac{\pi}{n}, \quad n \in \mathbb{Z}_{>0} , \tag{37}$$

we get, up to an additive constant, a simple effective action for the Wilson loops

$$S = -\frac{1}{\lambda}\mathcal{W}_1 + \sum_{n=1}^{\infty}\frac{1}{n}\mathcal{W}_n^2 \,. \tag{38}$$

Minimizing this action with respect to the $\mathcal{W}_n$ trivially gives $\mathcal{W}_1 = \frac{1}{2\lambda}$, $\mathcal{W}_{n\geq 2} = 0$, namely the strong coupling solution. However, for $\lambda < 1$ the corresponding matrices $\hat{\rho}^{(L)}$ are not all positive definite. Indeed, their eigenvalues are $\mu_k^{(L)} = 1 + \frac{1}{\lambda}\cos\frac{\pi k}{L+1}$, $k = 1 \ldots L+1$ that are not all positive for $\lambda < 1$. Therefore the correct problem to solve is

$$\text{Minimize} \quad S = -\frac{1}{\lambda}\mathcal{W}_1 + \sum_{n=1}^{L}\frac{1}{n}\mathcal{W}_n^2 \,, \tag{39}$$

$$\text{such that } \hat{\rho}^{(L)} = \frac{1}{L}\mathbb{T}[\mathcal{W}_0, \ldots, \mathcal{W}_L] \succeq 0 \,, \tag{40}$$

for some fixed L. This problem has the form known as Quadratic Programming and can be converted into a problem of Semi-Definite Programming (SDP) (see [21] and Appendix A) and solved by standard packages. Using the matlab cvx package [22] it is very easy to show numerically that for $L = 10$ the results for $\mathcal{W}_1 = u(\lambda)$ agree perfectly with the exact answer, and even for as low as $L = 6$ they are reasonably correct. Increasing further L one can get more precise values for $\mathcal{W}_1$ and also compute the other loops $\mathcal{W}_{n=1\ldots L}$, in good agreement with the exact answer. This approach provides an excellent numerical method purely in terms of the Wilson loop expectation values and valid for all values of the coupling. Unfortunately, in four dimensions there is no such simple action. For example, in [23] Jevicki and Sakita derived an effective action for Wilson loops and showed that it leads to the loop equations. However, it depends on a Jacobian that is only implicitly defined.

3.3. Approximate effective action

Although the results of the previously described numerical method are excellent already for small values of L we can consider a relatively low value, *e.g.* $L = 4$ and wonder if it is possible find an approximate value of u between the maximum and the minimum. This would be an approximation as opposed to the bounds that are analytical bounds. The low coupling phase is a low temperature phase and therefore should minimize the energy, equivalently maximize u. So, at small coupling we choose $u = u_{max}$ which indeed gives a very good answer, see Fig. 8. The large coupling or large temperature phase should have large entropy. In this case there is a simple entropy we can consider, namely the entropy associated to the matrix $\hat{\rho}^{(L)}$. Indeed, in the limit $\lambda \to 0$, all loops are given by $\mathcal{W}_n = 1$, $\hat{\rho}^{(L)}$ has one eigenvalue equal to one and all the others vanish. Namely it describes a pure state. Up to gauge transformations, the matrix U is the identity and we do not lose any information if we trace its powers. On the other hand when $\lambda \to \infty$ all loops vanish except $\mathcal{W}_0 = 1$. The matrix $\hat{\rho}$ is proportional to the identity and the entropy is a maximum. Namely, if we take traces of powers of U we lose a maximum amount of information for these configurations.

Therefore, the simple proposal is to maximize u for small coupling and maximize S_{WL} at large coupling. The results agrees with the exact solution better than the bounds. An even better result is obtained by defining an effective free energy

$$\mathcal{A} = -u + c\lambda \mathrm{Tr}\hat{\rho}^{(L)} \ln \hat{\rho}^{(L)} \,, \tag{41}$$

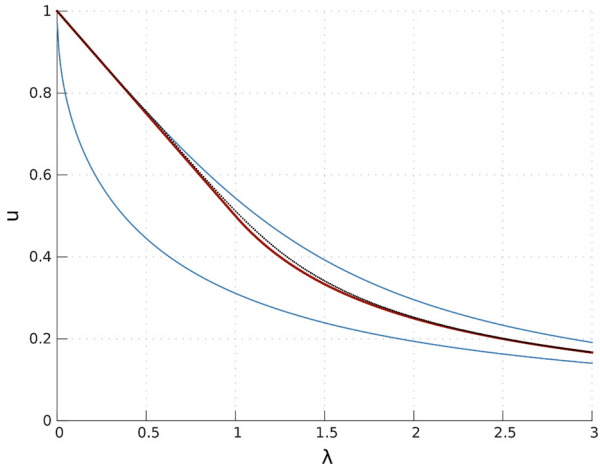

Fig. 9. For $L = 4$ the bounds are wide apart. However we get a good approximation (black curve) to the exact answer (red curve) using an effective action $S = -u + \frac{1}{2}\lambda \mathrm{Tr}\hat{\rho}^{(L)} \ln \hat{\rho}^{(L)}$. (For interpretation of the references to color in this figure, the reader is referred to the web version of this article.)

Table 1
Number of independent Wilson loops up to each given length L in four dimensions.

$L_{\max}$	# of Wilson loops
10	268
12	5324
14	142,105
16	4,483,136
18	152,322,746

where c is an adjustable constant of order one. We set $c = \frac{1}{2}$ because it seems to adjust the exact answer well (see Fig. 9) but we do not have a way to fix this constant from first principles. Of course the correct effective action is the one we gave in section 3.2 but here we wanted to find a simple effective action that could be used also in higher dimensions.

4. Four dimensional lattice

In four dimensions the numerical methods are similar as in two dimensions, the main difficulty being that the number of Wilson loops grows exponentially with the length, see Table 1. To handle that, we developed a computer program that listed all loops up to translations, rotations, reflections and cyclic permutations of the links up to length $L = 18$ although most calculations described below were done using loops up to length $L = 14$. It also computes the corresponding loop equations, strong coupling expansion, and the set of $\hat{\rho}$ matrices that have to be positive definite. Finally it provides output that can be further manipulated by computer algebra programs or standard packages such as cvx [22] or sdpa [24]. Let us now briefly describe different methods that can be used to solve the loop equation in different regimes and their usefulness.

4.1. Strong coupling expansion for plaquette expectation value

The strong coupling expansion for the Wilson loop can be done straight-forwardly using the loop equation [5] and therefore we use it to validate the computer program that determines the loop equation. Indeed writing the loop equation as

$$\mathcal{W}_i = \frac{1}{2\lambda}\delta_{i1} - \frac{1}{2\lambda}\mathbb{K}_{i\to j}\mathcal{W}_j - \mathbb{C}_{i\to jk}\mathcal{W}_j\mathcal{W}_k \,, \tag{42}$$

we obtain a simple solution as a series expansion

$$\mathcal{W}_i = \sum_{\ell=1}^{\infty} \frac{1}{\lambda^\ell}\mathcal{W}_i^{(\ell)} \,, \tag{43}$$

where

$$\mathcal{W}_i^{(1)} = \frac{1}{2}\delta_{i1} \tag{44}$$

$$\mathcal{W}_i^{(\ell)} = -\frac{1}{2}\mathbb{K}_{i\to j}\mathcal{W}_j^{(\ell-1)} - \mathbb{C}_{i\to jk}\sum_{\ell'=1}^{\ell-1}\mathcal{W}_j^{(\ell')}\mathcal{W}_k^{(\ell-\ell')} \,. \tag{45}$$

We obtain the expansion for the plaquette as

$$u = \frac{1}{2\lambda} + \frac{1}{8\lambda^5} + \mathcal{O}(\lambda^{-6}) \,. \tag{46}$$

Up to the computed order, the result agrees with [12,25] thus providing a way to validate our computer code.

4.2. Bootstrap-like method

The numerical method is a generalization of the one used in two dimensions. We consider all loops up to a given length L. Then we list all loop equations and extra equations associated with loops up to length $L-4$, namely all equations that do not involve loops longer than L and we construct all matrices $\hat{\rho}$ that do not contain loops longer than L. The loops of length $L-2$ and L are not determined by the equations. Setting them to zero allows us to recover the strong coupling solutions. Instead, we allow them to fluctuate under the condition that the $\hat{\rho}$ matrices are positive definite $\hat{\rho} \succeq 0$ and obtain an upper and lower bound on u. The bounds are not as stringent as in two dimensions, however at low coupling the upper bound, namely the one that minimizes the energy gives a good approximation to the actual solution. Let us first do this analytically for the simplest example, the loop equation for the plaquette in dimension $d \geq 3$. In the notation of Fig. 3, the equation is

$$2\lambda u = 1 + \mathcal{W}_2 + 2(d-2)\mathcal{W}_3 - \mathcal{W}_{20} - \mathcal{W}_{17} - 2(d-2)\mathcal{W}_{21} \,. \tag{47}$$

If we want to maximize u, we set $\mathcal{W}_2 = \mathcal{W}_3 = 1$, their maximum values and $\mathcal{W}_{20} = \mathcal{W}_{17} = \mathcal{W}_{21} = 2u^2 - 1$ their minimum values according to the previous subsection, eqs. (22) or (23). We then get an equation for the maximum

$$u^2 + \frac{\lambda}{2(d-1)}u - 1 = 0 \,. \tag{48}$$

One of the roots of this equation gives the upper bound, namely

$$u \leq \frac{1}{2}\left(-\frac{\lambda}{2(d-1)}+\sqrt{4+\frac{\lambda^2}{4(d-1)^2}}\right)=u_{\max}\,, \tag{49}$$

a bound valid for the Wilson action in a cubic lattice of any dimension $d \geq 3$. For $\lambda \to \infty$ we get $u_{\max} \simeq \frac{2(d-1)}{\lambda}$ and for $\lambda \to 0$, $u_{\max} \simeq 1 - \frac{\lambda}{4(d-1)}$. The bound has the right behavior but the coefficients are not right, as was somewhat expected from such crude bound. This calculation is simply an illustration that there is indeed a bound that follows from positivity of $\hat{\rho}$ and the loop equation. Similarly we can get a lower bound by choosing $\mathcal{W}_2 = \mathcal{W}_3 = 2u^2 - 1$, and $\mathcal{W}_{20} = \mathcal{W}_{17} = \mathcal{W}_{21} = 1$:

$$u \geq \frac{1}{2}\left(\frac{\lambda}{2d-3}-\sqrt{4+\left(\frac{\lambda}{2d-3}\right)^2}\right)=u_{\min}\,. \tag{50}$$

To go further we can use a numerical procedure that allows us to handle $\hat{\rho}$ matrices of size of order $10^3 \times 10^3$ and thousands of equations. The main obstacle is that the known numerical packages (see Appendix A) only deal with linear equations but the self-intersection term in the loop equation is quadratic. In this paper we only consider the case where the quadratic terms are proportional to u^2 or $u\,\mathcal{W}_n$ for some loop $\mathcal{W}_n$. Therefore, if we fix u the equations become linear and we can use standard packages to test if such value of u is allowed and thus determine the allowed range of u. Let us now discuss the numerical results.

4.3. *Linear case,* $L_{\max} = 8, 10$

Since we consider Wilson loops of maximum length given by $L_{\max} = 8, 10$ we can only impose the loop equation associated with loops up to length $L = 6$. Those loops do not have self intersections and therefore the loop equations are linear. In this case we can solve the problem using semi-definite programming in a direct way. For example using matlab and cvx [22] (see Appendix A) we find the bound depicted in Fig. 10. We already see that the results are reasonable for the maximum value of u at small coupling. The minimum value of u for $L_{8,10}$ turns out to be $u_{\min} = 0$ which is a correct but rather poor bound for the actual value of u. So, we consider now Wilson loops of larger length.

4.4. *Non-linear case in one variable,* $L_{\max} = 12, 14$

In this case we impose the loop equation up to length $L = 10$. Some of those loops self-intersect and we cannot use semi-definite programming directly. However, the self-intersection splits the loops into two whose total length is less or equal than $L = 10$ and therefore one of them at least has to be a plaquette. For that reason we propose a different semi-definite programming problem. We fix the value of u and define a new matrix $\hat{\rho}$ as

$$\hat{\rho}(t) = \hat{\rho} - t\mathbb{I}\,. \tag{51}$$

Now we maximize the value of t by allowing the loops other than the plaquette to take arbitrary values compatible with the loop equation. When the procedure finalizes, the value of t is equal to the lowest eigenvalue of $\hat{\rho}$ and it is the largest lowest eigenvalue that can be found for that fixed value of u. Thus, if $t_{max} < 0$ it is simply not possible to choose the other loops such that

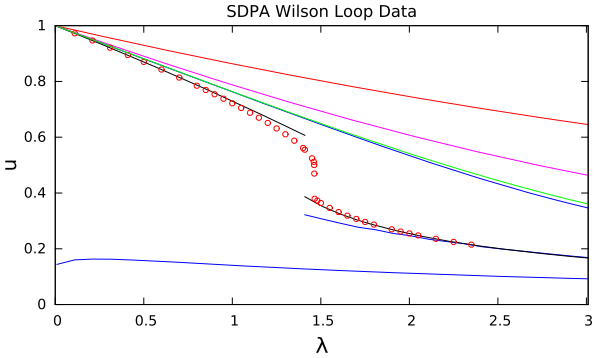

Fig. 10. Expectation value of the plaquette as a function of 't Hooft coupling in four dimensions. The black lines are the small and large coupling expansion and the circles the Monte Carlo simulation. The red and purple curves are the upper bounds from $L = 8, 10$ (see main text). The green line is the upper bound for $L = 12$ and the blue lines are the upper and lower bounds for $L = 14$, the best bounds we can presently get. At small coupling the upper bound is a reasonable approximation to the plaquette. At strong coupling the blue dashed curve is a good approximation and correspond to the maximum of t for $L = 14$ (see main text). (For interpretation of the colors in this figure, the reader is referred to the web version of this article.)

Table 2
Expectation value of the plaquette u for various values of the coupling λ. The three columns correspond to the upper bound obtained from the bootstrap method, the perturbative results [26] and the Monte Carlo calculation respectively. At small λ the bootstrap results are in good agreement with the perturbative and Monte Carlo results.

λ	Bootstrap	Perturbative	MC
0.01	0.9982	0.9975	0.9975
0.11	0.9738	0.9723	0.9725
0.21	0.9500	0.9466	0.9471
0.31	0.9262	0.9205	0.9212
0.41	0.9024	0.8941	0.8947
0.51	0.8786	0.8672	0.8676

the loop equation is satisfied and the matrix $\hat{\rho} \succeq 0$. Therefore this value of u is not allowed. In that way we can sweep the allowed values of u and determine the bounds on u and therefore on the energy. The results are depicted in Fig. 10 where the matrix $\hat{\rho}$ was truncated to an 800×800 size. The bounds are not close to each other as they were in two dimensions. At small coupling we minimize the energy and therefore choose the maximum value of u. Following the ideas discussed in section 3.3 for the two dimensional case, for large coupling we should maximize the entropy of the matrix $\hat{\rho}$. This is not an SDP problem and therefore we do a further approximation. Consider the value of u where $t_{max}(u)$ has a maximum. One can associate such point with a large value of entropy since increasing the minimum eigenvalue, with the trace being fixed, tends to make all eigenvalues similar. We are going to take such value of u as the best guess of the one that maximizes the entropy. This is depicted in Fig. 10 where we see that it is quite a good approximation at strong coupling. For comparison we present, in Table 2 the expectation values of the plaquettes for various values of the coupling, from our results, the perturbative results and Monte Carlo calculations.

4.5. Small coupling expansion

As a further check, we can do a small coupling expansion by linearly expanding all loops as

$$\mathcal{W}_n = 1 - \lambda w_n + \mathcal{O}(\lambda^2) \,, \tag{52}$$

and finding bounds on w_n. Using sdpa for loops up to length $L = 12$ we find for the plaquette $w_1 \geq 0.238$ and for $L = 14$ $w_1 \geq 0.2495$ in agreement with the known value $w_1 = \frac{1}{4}$ [26].

4.6. Lattice simulation

Numerical simulations of the large-N lattice pure gauge theory are well-known since the work of Creutz and Moriarty [27], for more recent work see *e.g.* [28]. Here we find it useful to perform such simulations as a way to check the previous results and to better understand the loop equation. Our Monte Carlo simulation used the Metropolis Algorithm to produce an ensemble of uncorrelated configurations using the partition function in eqs. (1), (2). In order to ensure that the results were properly thermalized we allowed the simulation to run for 20000 updates before saving configurations. Each update consisted of 10 "hits" on each link. A hit is one attempt to move the link through the phase space. After thermalization, one configuration every 100 updates was saved until a total of 300 configurations were collected. Binning showed that the correlation time of the system was around 400 updates between saves. Error was calculated via the bootstrap method and we found that for Wilson Loops up to length 10 the error in the expectation value was around 10^{-5} for lattices of size 8^4. The simulation was programmed using CUDA on GeForce GTX 980s. The expectation value of each Wilson loop was computed by averaging over configurations and over all possible positions and rotations of the loop. This allowed us to check the loop equations validity explicitly through the Monte Carlo Simulation. The finite N loop equations (10) were checked to be valid for $3 \leq N \leq 10$. We want to emphasize that for the equation to be valid for the $SU(N)$ case the right-hand side of eq. (10) is necessary. Furthermore, the large-N loop equations (11) were satisfied up to order $\frac{1}{N^2}$ corrections.

Finally, we can compare the simulation and the bootstrap results for loops other than the plaquette. In Fig. 11 the results for loops $\mathcal{W}_2$, $\mathcal{W}_3$, $\mathcal{W}_4$ (see Fig. 3) are displayed. The agreement is reasonable at small coupling $\lambda \lesssim 0.5$ if we used the solution that minimizes the Energy (maximizes u), in agreement with our previous discussion. For larger values of the coupling but below the transition the agreement is qualitative in the sense that the larger loops have smaller values than the plaquette. In the strong coupling phase, we choose the solution that maximizes t but the previously found agreement (Fig. 10) for the plaquette does not extend to the other loops. Clearly, the well-known strong coupling expansion is still the best method in this region.

5. $\mathcal{N} = 4$ SYM

The case of $\mathcal{N} = 4$ SYM is particularly important since it has a dual description as a string theory [1]. In the context of its relation to string theory and more precisely with the AdS/CFT correspondence, the loop equation has been formulated and studied in [29]. Studying the theory in the lattice should allow a different method of computation and possible strong coupling calculations based on the gauge theory side of the correspondence. In the rest of this section we briefly describe how the ideas we developed for pure YM could be implemented but, for concrete calculations, at the moment we restrict ourselves to the bosonic sector leaving the study of the full theory for future work.

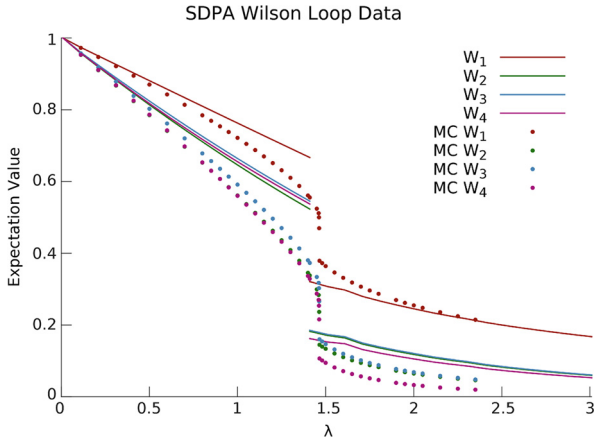

Fig. 11. Expectation value of loops $u = \mathcal{W}_1, \mathcal{W}_2, \mathcal{W}_3, \mathcal{W}_4$ (see Fig. 3) are displayed as a function of the 't Hooft coupling λ.

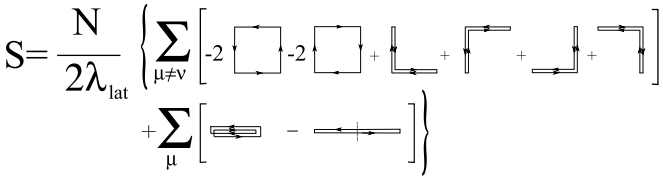

Fig. 12. The Lattice action for $\mathcal{N} = 4$ SYM can be written in terms of Wilson loops, the figure shows the bosonic sector that we use in the main text. The indices $\mu, \nu = 1 \ldots 5$ since the $A4^*$ lattice has five fundamental vectors.

A lattice theory that has the correct continuum theory without the need for fine-tuning is described in [30]. Here we use that formulation but follow the notation found in the paper [31]. For brevity we do not explain details and refer the reader to that work for explanation of the notation and properties of the theory. The main property is that such formulation preserves one twisted [32] scalar supercharge and possesses BPS Wilson loops although more restricted than the continuum theory. For our purposes another important property is that the action can be formulated entirely in terms of generalized Wilson loops, namely using loops with fermionic links and/or sites. In this way, the form of the loop equation given in (14) is valid using the appropriate supersymmetric action [31]. However, we have not worked out the correct generalization of the $\hat{\rho}$ matrices to the fermionic sector and therefore here we restrict ourselves to the bosonic sector described by the simpler action

$$S = \frac{N}{2\lambda_{lat}} \sum_x \mathrm{Tr} \left(\mathcal{F}^{\dagger}_{ab}(x) \mathcal{F}_{ab}(x) + \frac{1}{2} \left(\bar{\mathcal{D}}^{(-)}_a \mathcal{U}_a(x) \right)^2 \right) . \tag{53}$$

This action, thought as a linear combination of Wilson loops is depicted in Fig. 12. In order to obtain the loop equations we must vary individual links. However, the scalar and the gauge fields are twisted together which means that the matrices $\mathcal{U}_a(x) \in GL(N, \mathbb{C})$ and therefore the links and their daggers must be treated independently:

$$\mathcal{U}_a(x) \Rightarrow (1 + i\epsilon_a(x))\mathcal{U}_a(x) \tag{54}$$

$$\bar{\mathcal{U}}_a(x) \Rightarrow \bar{\mathcal{U}}_a(x)(1 - i\bar{\epsilon}_a(x)) \, . \tag{55}$$

Table 3
Wilson loop expectation values used to check the loop equation (56).

	$N=2$			$N=3$		
$\lambda =$	0.8	1.0	1.2	0.8	1.0	1.2
$\mathcal{W}_1$	0.01158	0.01451	0.01740	0.01151	0.01440	0.01724
$\mathcal{W}_2$	0.00241	0.00377	0.00543	0.00241	0.00377	0.00540
$\mathcal{W}_3$	0.00052	0.00082	0.00118	0.00048	0.00075	0.00109
$\mathcal{W}_4$	0.00026	0.00041	0.00059	0.00026	0.00040	0.00057
$\mathcal{W}_5$	0.00023	0.00036	0.00051	0.00023	0.00036	0.00051
$\mathcal{W}_6$	0.00205	0.00321	0.00462	0.00206	0.00321	0.00462
$\mathcal{W}_7$	0.00218	0.00343	0.00494	0.00219	0.00341	0.00489
$\mathcal{W}_8$	0.00525	0.00823	0.01184	0.00520	0.00812	0.01164
$\mathcal{W}_9$	0.00330	0.00518	0.00745	0.00322	0.00503	0.00723
Eq.	−0.00004	−0.00004	−0.00003	0.00002	−0.00003	−0.00001

This implies that in eq. (14), the intersection of the action with the loop is non-zero only for links oriented in the same direction, the same is true for a loop self-intersection. Since the gauge group is $U(N)$ the ϵ's do not have the constraint that they have to be traceless simplifying the finite N Loop Equations. The matrices $\hat{\rho}$ can be constructed similarly since we associate the hermitian conjugate of $\mathcal{U}_a$ to a link traversed in the opposite direction. Notice that in this case the property that a backtracking path can be eliminated is no longer true. In fact such backtracking paths correspond to the insertion of scalar fields. Now we check the loop equation using a numerical simulation and leave the full exploration of the bootstrap method for future work.

5.1. Monte Carlo simulation

We used the parallel code developed by Schaich and DeGrand [33], based on the previous work by Catterall and Joseph [34] to simulate the latticized Euclidean theory. The code allows for a simple way to reduce to the bosonic sector, *i.e.* to the six scalars and four gauge fields that in this formulation live on the links. The lattice is taken to be an A_4^* lattice which contains the permutation group S_5, the largest finite subgroup of the four dimensional rotation symmetry. In order to preserve a subgroup of the SUSY Algebra, the Euclidean–Lorentz and R symmetry groups are twisted into $SO(4)_E \otimes SO(6)_R \to SO(4)' \otimes U(1)$. With this twisting the lattice theory is invariant under one supercharge out of the full sixteen. The continuum limit should restore the full sixteen supercharges without fine-tuning.

To test the loop equations we considered the loop equation associated with the plaquette and found that it is satisfied up to four digits which is within the numerical accuracy of the simulation. The test was done for U(2) and U(3) gauge groups and for $\lambda_{lat} = 0.8, 1.0, 1.2$ on 8^4 lattices. The results are presented in Table 3. The loop equation necessary for the plaquette with the pure bosonic action is given by eq. (56) and seen pictorial in Fig. 13

$$\frac{1}{2\lambda_{lat}}(-\mathcal{W}_2 - \mathcal{W}_3 - \mathcal{W}_4 - 6\mathcal{W}_5 + 6\mathcal{W}_6 + \mathcal{W}_7 + \mathcal{W}_8 + \mathcal{W}_9) - \mathcal{W}_1 = 0\,. \tag{56}$$

This concludes our brief study of the $\mathcal{N}=4$ case. The next step, that we leave for future work, would be to formulate the loop equation for the full $\mathcal{N}=4$ theory, namely including fermions and appropriately generalize the positivity constraints that are necessary to implement our numerical method.

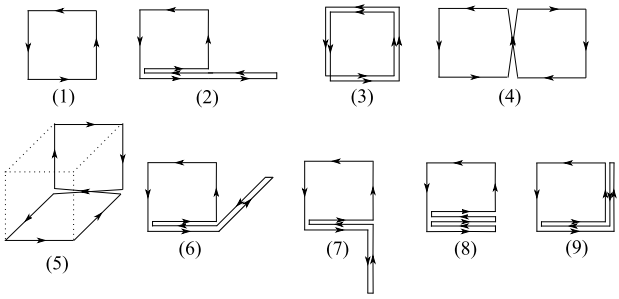

Fig. 13. The Wilson loops necessary for the plaquette loop equation of the bosonic $\mathcal{N} = 4$ SYM action.

6. Conclusions

The loop equation has been traditionally seen as a promising way to describe gauge theories in terms of gauge invariant quantities. In this paper we agree with this perspective but also point out that such equation has infinite solutions that have to be constrained by the condition that certain matrices are positive definite. At strong coupling such extra conditions are not necessary and therefore seem to have been largely ignored. On the other hand, in the physically relevant region of small coupling such conditions are crucial to obtain the correct solution. In fact they also give many constraints and properties that are actually independent of the action. In two dimensions this leads to a simple numerical procedure that reproduces the exact solution for any coupling. This method can potentially be used for other two dimensional actions where the exact solution is not known but, more importantly, it can be extended to higher dimensions. The simple idea is that given two points in space and a set of open lines $\ell = 1 \dots L$ between them, we can define an $L \times L$ matrix of closed loops where the entry $\ell\ell'$ is the expectation value of the closed loop obtained by going along path ℓ and returning along path ℓ'. Such matrix has to be positive definite and can be considered as a reduced density matrix due to tracing over the color indices. Its entropy measures how much information is lost by taking the traces and gives a qualitative idea of the entropy of the system. The reason is that the entropy of the matrix $\hat{\rho}$ vanishes in the ground state when all links are equal to the identity (up to gauge transformations) and is maximal at large coupling when the links fluctuate randomly.

Numerically we implement a procedure to solve the loop equation under the condition that the constraints are satisfied. It reproduces known results from Monte Carlo simulations but cannot be considered an improvement. It is possible that more computational resources could lead to better results especially in the small coupling region relevant to the continuum limit. Also, it might be possible to improve the choice of the constraints, namely the matrix $\hat{\rho}$, and/or use improved actions that approach the continuum limit faster. It is also interesting to extend this method to other theories whose action can be formulated entirely in terms of closed loops. One such theory is $\mathcal{N} = 4$ SYM, of particular importance since it plays a central role in the AdS/CFT correspondence. Initial steps in this direction suggest that the method can be applied but requires a better understanding of the fermionic loops. Another system to consider is three dimensional Yang–Mills where there are other approaches [35,36].

Acknowledgements

This work was supported in part by the DOE through grant DE-SC0007884. We are very grateful for numerous discussions with P. Vieira, S. Catterall, D. Schaich on the matters of this

work and/or lattice gauge theory in general. Also S. Catterall and D. Schaich graciously provided their lattice code allowing us to check the loop equations in the bosonic sector of $\mathcal{N} = 4$ SYM. We are also grateful to D. Minic and A. Jevicki for useful comments on a previous version of this work. P.D.A. would like to thank the Wigner GPU Laboratory at the Wigner Research Center for Physics (Budapest, Hungary) for providing GPUs computer resources. He would also like to thank G.G. Barnaföldi, M.F. Nagy-Egri, D. Berényi, and Z. Bajnok for helpful discussions. M.K. wants to thank the hospitality of the Perimeter Institute, Waterloo, CA and the SAIFR Institute (São Paulo, Brazil), while part of this work was being done.

Appendix A. Semi-definite programming (SDP)

Semi-definite programming [21] is a type of optimization problem that has been the focus of a lot of attention recently in relation to problems in finance, engineering, and more recently has proved invaluable in the bootstrap program of conformal field theories (see *e.g.* [7]).

It can be stated very simply as:

Given m real numbers $c_{i=1\ldots m} \in \mathbb{R}$ and m real, symmetric $n \times n$ matrices $\mathbb{F}_{i=0\ldots m} \in \mathbb{R}^{n\times n}$, find $x_{i=1\ldots m} \in \mathbb{R}$ that minimize $\sum_{i=1}^{m} c_i x_i$ under the constraint that $\mathbb{X} = \sum_{i=1}^{m} x_i \mathbb{F}_i - \mathbb{F}_0$ is positive semi-definite ($\mathbb{X} \succeq 0$).

The main observation in this field is that the space of semi-definite matrices is a convex cone in the space of all symmetric $n \times n$ matrices. Indeed, given two positive semi-definite matrices $\mathbb{X}_{1,2} \succeq 0$, namely $y^t \mathbb{X}_{1,2} y \geq 0,\ \forall\ y \in \mathbb{R}^n$, then it is clear that $y^t(\alpha_1 \mathbb{X}_1 + \alpha_2 \mathbb{X}_2) y \geq 0$ for any real $\alpha_{1,2} \geq 0$. Thus, $\alpha_1 \mathbb{X}_1 + \alpha_2 \mathbb{X}_2 \succeq 0,\ \forall\ \alpha_{1,2} \geq 0$ showing that positive semi-definite matrices form a convex cone. The condition that $\mathbb{X}$ belongs to the linear subspace generated by the $\mathbb{F}_{i=1\ldots m}$ shifted by $\mathbb{F}_0$ defines an intersection between this hyperplane and the semi-definite cone. This is a convex region over which we minimize a linear function. Therefore, the minimum is unique and should be located at the boundary of the domain, namely when the matrix $\mathbb{X}$ has at least one zero eigenvalue. The problem is then very similar to the more traditional problem of linear programming where one minimizes a linear function $\sum_{i=1}^{m} c_i x_i$ over the convex cone $y_{\ell=1\ldots n} \geq 0$ where the $y_\ell = \sum_{i=1}^{m} a_{\ell i} x_i$ for some given coefficients $\alpha_{\ell i}$.

There are many other problems that can be reduced to an SDP problem. For example, in section 3.2 we need to solve

$$\begin{aligned} &\text{Minimize} \quad S = -\frac{1}{\lambda}\mathcal{W}_1 + \sum_{n=1}^{L} \frac{1}{n}\mathcal{W}_n^2 \,, \\ &\text{such that } \hat{\rho}^{(L)} = \frac{1}{L}\mathbb{T}[\mathcal{W}_0, \ldots, \mathcal{W}_L] \succeq 0 \,, \end{aligned} \tag{57}$$

this is problem of quadratic programming that can be reduced to an SDP problem by defining a new variable t and imposing

$$-\frac{1}{\lambda}\mathcal{W}_1 + \sum_{n=1}^{L} \frac{1}{n}\mathcal{W}_n^2 \leq t \,, \tag{58}$$

or equivalently

$$S_M = \begin{pmatrix} t & (u-\frac{1}{2\lambda}) & \frac{\mathcal{W}_2}{\sqrt{2}} & \frac{\mathcal{W}_3}{\sqrt{3}} & \dots \\ (u-\frac{1}{2\lambda}) & 1 & 0 & 0 & \dots \\ \frac{\mathcal{W}_2}{\sqrt{2}} & 0 & 1 & 0 & \dots \\ \frac{\mathcal{W}_3}{\sqrt{3}} & 0 & 0 & 1 & \dots \\ \vdots & \vdots & \vdots & \vdots & \ddots \end{pmatrix} \succeq 0 \,. \tag{59}$$

Thus the problem (57) is equivalent to

$$\text{Minimize } t, \text{ such that } \ \rho^{(L)} \succeq 0, \ S_M \succeq 0 \,. \tag{60}$$

Once the problem has been casted as an SDP problem, there are several available packages that can be used to solve it. We found that for rapid development of small problems the matlab package cvx [22] was very convenient and, for larger problems sdpa [24] was a good choice.

References

[1] J. Maldacena, The large N limit of superconformal field theories and supergravity, Adv. Theor. Math. Phys. 2 (1998) 231, Int. J. Theor. Phys. 38 (1998) 1113, arXiv:hep-th/9711200;
S.S. Gubser, I.R. Klebanov, A.M. Polyakov, Gauge theory correlators from non-critical string theory, Phys. Lett. B 428 (1998) 105, arXiv:hep-th/9802109;
E. Witten, Anti-de Sitter space and holography, Adv. Theor. Math. Phys. 2 (1998) 253, arXiv:hep-th/9802150.

[2] G.'t Hooft, Nucl. Phys. B 72 (1974) 461;
G.'t Hooft, Nucl. Phys. B 75 (1974) 461.

[3] Y.M. Makeenko, A.A. Migdal, Exact equation for the loop average in multicolor QCD, Phys. Lett. B 88 (1979) 135;
Y.M. Makeenko, A.A. Migdal, Selfconsistent areas law in QCD, Phys. Lett. B 97 (1980) 253;
S.R. Wadia, On the Dyson–Schwinger equations approach to the large N limit: model systems and string representation of Yang–Mills theory, Phys. Rev. D 24 (1981) 970;
G.F. De Angelis, D. de Falco, F. Guerra, Lattice gauge models in the strong coupling regime, Lett. Nuovo Cimento 19 (1977) 55;
F. Guerra, R. Marra, G. Immirzi, Strong coupling expansion for lattice Yang–Mills fields, Lett. Nuovo Cimento 23 (1978) 237;
A.M. Polyakov, Gauge fields as rings of glue, Nucl. Phys. B 164 (1979) 171;
T. Eguchi, Strings in U(N) lattice gauge theory, Phys. Lett. B 87 (1979) 91;
B. Sakita, Field theory of strings as a collective field theory of U(N) gauge field, Phys. Rev. D 21 (1980) 1067;
D. Foerster, Yang–Mills theory – a string theory in disguise, Phys. Lett. B 87 (1979) 83;
A. Jevicki, B. Sakita, The quantum collective field method and its application to the planar limit, Nucl. Phys. B 165 (1980) 511.

[4] A.A. Migdal, Loop equations and 1/N expansion, Phys. Rep. 102 (1983) 199.

[5] G. Marchesini, Loop dynamics for gauge theories: a numerical algorithm, Nucl. Phys. B 239 (1984) 135;
G. Marchesini, E. Onofri, Convergence of the iterative solution of loop equations in planar QCD in two-dimensions, Nucl. Phys. B 249 (1985) 225.

[6] R. Rattazzi, V.S. Rychkov, E. Tonni, A. Vichi, Bounding scalar operator dimensions in 4D CFT, J. High Energy Phys. 0812 (2008) 031, http://dx.doi.org/10.1088/1126-6708/2008/12/031, arXiv:0807.0004 [hep-th];
V.S. Rychkov, A. Vichi, Universal constraints on conformal operator dimensions, Phys. Rev. D 80 (2009) 045006, http://dx.doi.org/10.1103/PhysRevD.80.045006, arXiv:0905.2211 [hep-th].

[7] F. Kos, D. Poland, D. Simmons-Duffin, Bootstrapping the $O(N)$ vector models, J. High Energy Phys. 1406 (2014) 091, arXiv:1307.6856 [hep-th].

[8] M.F. Paulos, J. Penedones, J. Toledo, B.C. van Rees, P. Vieira, The S-matrix bootstrap II: two dimensional amplitudes, arXiv:1607.06110 [hep-th];
M.F. Paulos, J. Penedones, J. Toledo, B.C. van Rees, P. Vieira, The S-matrix bootstrap I: QFT in AdS, arXiv:1607.06109 [hep-th].

[9] A. Jevicki, O. Karim, J.P. Rodrigues, H. Levine, Loop space Hamiltonians and numerical methods for large N gauge theories, Nucl. Phys. B 213 (1983) 169;
A. Jevicki, O. Karim, J.P. Rodrigues, H. Levine, Loop space Hamiltonians and numerical methods for large N gauge theories. 2, Nucl. Phys. B 230 (1984) 299;
A. Jevicki, B. Sakita, Loop space representation and the large N behavior of the one plaquette Kogut–Susskind Hamiltonian, Phys. Rev. D 22 (1980) 467.
[10] A. Jevicki, B. Sakita, The quantum collective field method and its application to the planar limit, Nucl. Phys. B 165 (1980) 511, http://dx.doi.org/10.1016/0550-3213(80)90046-2.
[11] L.G. Yaffe, Large N limits as classical mechanics, Rev. Mod. Phys. 54 (1982) 407.
[12] J.M. Drouffe, J.B. Zuber, Strong coupling and mean field methods in lattice gauge theories, Phys. Rep. 102 (1983) 1.
[13] Y. Makeenko, Methods of Contemporary Gauge Theory, Cambridge Monographs on Mathematical Physics, Cambridge University Press, 2002.
[14] M. Campostrini, The large N phase transition of lattice SU(N) gauge theories, Nucl. Phys. Proc. Suppl. 73 (1999) 724.
[15] K.G. Wilson, Confinement of quarks, Phys. Rev. D 10 (1974) 2445.
[16] A.A. Migdal, Properties of the loop average in QCD, Ann. Phys. 126 (1980) 279.
[17] D.J. Gross, E. Witten, Possible third order phase transition in the large N lattice gauge theory, Phys. Rev. D 21 (1980) 446;
S.R. Wadia, A study of U(N) lattice gauge theory in 2-dimensions, arXiv:1212.2906 [hep-th] (unpublished 1979 EFI (U. Chicago) preprint).
[18] D. Friedan, Some nonabelian toy models in the large N limit, Commun. Math. Phys. 78 (1981) 353, http://dx.doi.org/10.1007/BF01942328.
[19] Albrecht Böttcher, Bernd Silbermann, Toeplitz Determinants, Analysis of Toeplitz Operators, Springer-Verlag, Berlin, 1990, p. 525. See also: Toeplitz and Circulant Matrices: A Review (Foundations and Trends in Communications and Information Theory) by Robert M. Gray, Now Publishers Inc (2006).
[20] I.S. Gradshteyn, I.M. Ryzhik, Table of Integrals Series and Products, sixth edition, Academic Press, San Diego, CA, USA, London, UK, 2000.
[21] L. Vandenberghe, S. Boyd, SIAM Rev. 38 (1) (March 1996) 49–95.
[22] Michael Grant, Stephen Boyd, CVX: Matlab software for disciplined convex programming, version 2.0 beta, http://cvxr.com/cvx, September 2013;
Michael Grant, Stephen Boyd, Graph implementations for nonsmooth convex programs, in: V. Blondel, S. Boyd, H. Kimura (Eds.), Recent Advances in Learning and Control (a Tribute to M. Vidyasagar), in: Lecture Notes in Control and Information Sciences, Springer, 2008, pp. 95–110, http://stanford.edu/~boyd/graph_dcp.html.
[23] A. Jevicki, B. Sakita, Collective field approach to the large N limit: Euclidean field theories, Nucl. Phys. B 185 (1981) 89.
[24] Makoto Yamashita, Katsuki Fujisawa, Mituhiro Fukuda, Kazuhiro Kobayashi, Kazuhide Nakta, Maho Nakata, Latest developments in the SDPA family for solving large-scale SDPs, in: Miguel F. Anjos, Jean B. Lasserre (Eds.), Handbook on Semidefinite, Cone and Polynomial Optimization: Theory, Algorithms, Software and Applications, Springer, NY, USA, 2011, pp. 687–714, Chapter 24;
Makoto Yamashita, Katsuki Fujisawa, Kazuhide Nakata, Maho Nakata, Mituhiro Fukuda, Kazuhiro Kobayashi, Kazushige Goto, A High-Performance Software Package for Semidefinite Programs: SDPA 7, Research Report B-460, Dept. of Mathematical and Computing Science, Tokyo Institute of Technology, Tokyo, Japan, September 2010;
Makoto Yamashita, Katsuki Fujisawa, Masakazu Kojima, Implementation and evaluation of SDPA 6.0 (SemiDefinite Programming Algorithm 6.0), Optim. Methods Softw. 18 (2003) 491–505.
[25] V.A. Kazakov, U(infinity) lattice gauge theory as a free lattice string theory, Phys. Lett. B 128 (1983) 316;
I.K. Kostov, Multicolor QCD in terms of random surfaces, Phys. Lett. B 138 (1984) 191;
I.K. Kostov, On the random surface representation of U (infinite) lattice gauge theory, Phys. Lett. B 147 (1984) 445.
[26] U.M. Heller, F. Karsch, One loop perturbative calculation of Wilson loops on finite lattices, Nucl. Phys. B 251 (1985) 254.
[27] M. Creutz, K.J.M. Moriarty, Phase transition in SU(6) lattice gauge theory, Phys. Rev. D 25 (1982) 1724.
[28] H. Meyer, M. Teper, Confinement and the effective string theory in $SU(N \to \infty)$: a lattice study, J. High Energy Phys. 0412 (2004) 031.
[29] A.M. Polyakov, String theory and quark confinement, Nucl. Phys. Proc. Suppl. 68 (1998) 1;
A.M. Polyakov, V.S. Rychkov, Gauge field strings duality and the loop equation, Nucl. Phys. B 581 (2000) 116;

A.M. Polyakov, V.S. Rychkov, Loop dynamics and AdS / CFT correspondence, Nucl. Phys. B 594 (2001) 272;
N. Drukker, A new type of loop equations, J. High Energy Phys. 9911 (1999) 006.

[30] S. Catterall, D.B. Kaplan, M. Unsal, Exact lattice supersymmetry, Phys. Rep. 484 (2009) 71;
S. Catterall, D. Schaich, P.H. Damgaard, T. DeGrand, J. Giedt, $N = 4$ supersymmetry on a space–time lattice, Phys. Rev. D 90 (6) (2014) 065013;
S. Catterall, Dirac–Kahler fermions and exact lattice supersymmetry, PoS LAT 2005 (2006) 006;
D.B. Kaplan, M. Unsal, A Euclidean lattice construction of supersymmetric Yang–Mills theories with sixteen supercharges, J. High Energy Phys. 0509 (2005) 042.

[31] S. Catterall, J. Giedt, A. Joseph, Twisted supersymmetries in lattice $\mathcal{N} = 4$ super Yang–Mills theory, J. High Energy Phys. 1310 (2013) 166.

[32] N. Marcus, The other topological twisting of $N = 4$ Yang–Mills, Nucl. Phys. B 452 (1995) 331.

[33] D. Schaich, T. DeGrand, Parallel software for lattice $N = 4$ supersymmetric Yang–Mills theory, Comput. Phys. Commun. 190 (2015) 200.

[34] S. Catterall, A. Joseph, An object oriented code for simulating supersymmetric Yang–Mills theories, Comput. Phys. Commun. 183 (2012) 1336.

[35] R.G. Leigh, D. Minic, A. Yelnikov, Solving pure QCD in $2 + 1$ dimensions, Phys. Rev. Lett. 96 (2006) 222001;
R.G. Leigh, D. Minic, A. Yelnikov, On the spectrum of Yang–Mills theory in $2 + 1$ dimensions, analytically, Can. J. Phys. 85 (2007) 687.

[36] D. Karabali, V.P. Nair, A gauge-invariant Hamiltonian analysis for non-Abelian gauge theories in $(2 + 1)$ dimensions, Nucl. Phys. B 464 (1996) 135;
D. Karabali, V.P. Nair, On the origin of the mass gap for non-Abelian gauge theories in $(2 + 1)$ dimensions, Phys. Lett. B 379 (1996) 141;
D. Karabali, C.j. Kim, V.P. Nair, Planar Yang–Mills theory: Hamiltonian, regulators and mass gap, Nucl. Phys. B 524 (1998) 661;
D. Karabali, C.j. Kim, V.P. Nair, On the vacuum wave function and string tension of Yang–Mills theories in $(2 + 1)$ dimensions, Phys. Lett. B 434 (1998) 103;
D. Karabali, C.j. Kim, V.P. Nair, Manifest covariance and the Hamiltonian approach to mass gap in $(2 + 1)$-dimensional Yang–Mills theory, Phys. Rev. D 64 (2001) 025011.